Geophys. J. R. astr. Soc. (1981) **66**, 579–596

Thermodynamic parameters in the Earth as determined from seismic profiles

J. M. Brown *Department of Geophysics, Texas A & M University, College Station, Texas 77843, USA*

T. J. Shankland *Geophysics Group, MS 977, University of California, Los Alamos National Laboratory, Los Alamos, New Mexico 87545, USA*

Received 1980 October 28; in original form 1979 September 4

Summary. A Debye model using two cut-off frequencies corresponding to compressional and shear velocities is used to calculate mineral entropies. This model permits entropy and heat capacity in the Earth to be calculated from seismic profiles, and iteration yields temperature profiles along an isentrope. With an adiabatic temperature profile it is possible to obtain Grüneisen's parameter and thermal expansion as a function of depth. Only in the lower mantle is the calculated Grüneisen's parameter along an isentrope approximately proportional to volume.

Introduction

Defining the thermal state of the Earth's interior has been a constant concern of geophysics. Earth models provide the primary data for this description: pressure, density, and two elastic moduli. However, pressure and density do not uniquely define a thermodynamic state. Other parameters, e.g. composition, heat capacity, thermal expansion, and/or Grüneisen's parameter are necessary, and at present these quantities must be determined from the elastic properties.

A correct approach to calculation of thermodynamic quantities starting from elastic properties involves lattice dynamical methods. Information regarding crystal symmetry, interatomic coupling parameters, and their volume dependences must be included. However, the technique is analytically complex and requires input not directly available for the Earth's interior. In the absence of a complete model, many authors have formulated or justified their work in terms of the Debye model (e.g. O. L. Anderson 1979a; Shankland 1972; Mao 1974; Shaw 1976) even though this model makes a number of simplifying assumptions concerning the energy states of a solid. However, the Debye model persists in geophysics because the information required for thermodynamic calculations – elastic wave velocities and density – is just that provided by seismic earth models.

This paper further investigates the usefulness of the Debye model for describing the thermodynamic state of the Earth. First, a Debye model having cut-off frequencies for both compressional and shear waves is used to calculate entropy for a variety of solids. This

method is a generalization (Brillouin 1953) of the standard Debye model in which shear and compressional velocities are averaged to produce a single cut-off frequency. Entropies calculated using two cut-off frequencies are shown to match tabulated entropies of crystals with less scatter than do single-frequency calculations.

This approach is then applied to the Earth using seismic velocities and densities. Under the assumption that to first order the lower mantle and core have an adiabatic temperature profile, temperatures within the Earth may be calculated and other thermal properties follow from standard thermodynamic identities. This approach reverses the usual method in which an adiabatic profile is calculated from parameters obtained from laboratory or theoretical studies.

Entropy calculations

The entropy of a solid is a sum of structural and vibrational terms. Contributions to structural disorder include vacant lattice sites, interstitial atoms, impurities, and substitutions; magnetic effects can also contribute. The vibrational entropy term will be calculated here, although mention will be made later concerning other contributions.

Construction of thermodynamic functions relies on description of the distribution of quantized (vibrational) energy states in a solid. Detailed treatments of the problem are found in numerous sources (Smith 1969; Brillouin 1953). Results for the Debye model are given here along with a brief discussion.

For a Debye model with two cut-off frequencies the entropy is (Brillouin 1953, Chapter VII)

$$S_{\text{Debye}} = -R \ln [\exp(x_p) - 1] + \frac{4R}{x_p^3} \int_0^{x_p} \frac{\exp(x)\, x^3}{\exp(x) - 1}\, dx - 2R \ln [\exp(x_s) - 1] + \frac{8R}{x_s^3} \int_0^{x_s} \frac{\exp(x)\, x^3}{\exp(x) - 1}\, dx. \quad (1)$$

where

$$x_p = h \left(\frac{9N}{4\pi} \frac{\rho}{\bar{m}}\right)^{1/3} V_p/kT = \theta_p/T$$

$$x_s = h \left(\frac{9N}{4\pi} \frac{\rho}{\bar{m}}\right)^{1/3} V_s/kT = \theta_s/T$$

h = Planck's constant,
R $\equiv Nk$ – gas constant,
N ≡ Avogadro's number,
k ≡ Boltzman's constant,
ρ ≡ density,
$\bar{m}$ ≡ mean atomic weight,
T ≡ absolute temperature,
V_p, V_s ≡ compressional, transverse elastic wave velocities,
θ_p, θ_s ≡ compressional, transverse Debye temperatures.

Heat capacity follows as

$$T \left(\frac{\partial S}{\partial T}\right)_V = C_{V_{\text{Debye}}} = \frac{3R}{x_p^3} \int_0^{x_p} \frac{x^4 \exp(x)}{[\exp(x) - 1]^2} + \frac{6R}{x_s^3} \int_0^{x_s} \frac{x^4 \exp(x)}{[\exp(x) - 1]^2}\, dx. \quad (2)$$

These equations imply two peaks in the distribution of energy states, one for compressional, and one for shear modes. Brillouin (1953) showed agreement between this distribution and that found for many solids. While a number of simplifications are used in this model, neglect of optical modes of vibration is usually responsible for the most substantial deviations between theory and experiment (e.g. Smith 1969). Since the Debye frequency distribution is based on non-dispersive acoustic modes that are governed by elastic-wave velocities, it is important to determine the conditions under which neglect of optic modes becomes important.

All polyatomic and those monoatomic crystals with more than one atom per unit cell have optical modes. A distinction may be made, however, between crystals with optical modes at frequencies much larger than acoustic cut-off frequencies and those with optical modes within the range of the acoustic modes. Apart from anharmonic effects either a Debye or a more complex model can predict entropies per atom at temperatures near the highest characteristic temperature, i.e. where all modes are saturated and heat capacity is constant. In the former case of very high frequency optic modes a Debye model might be expected to be a poor description because some modes are unsaturated, while in the latter case a Debye model might be adequate.

This difference may be illustrated by two common minerals, quartz and halite. α-quartz provides an extreme example in that its compression occurs through distortions of the angles between relatively undistorted silicon tetrahedra (Hazen 1977; Jorgensen 1978) while the highest optical mode involves breathing mode vibrations of a tetrahedron where the restoring forces are much greater. Thus, the longitudinal Debye cut-off frequency is only 539 cm^{-1},

Table 1. Entropy values and Debye heat capacities at standard temperature and pressure in J/K gm atom.

Materials and Structures	$S_{experimental}$	S_{Debye}	($S_{experimental}$ - Debye)	$C_{V_{Debye}}$
Alkali Halides				
LiF	17.8[a]	15.4[c]	2.4	18.9
LiCl	29.1[a]	25.9[c]	3.2	22.3
LiBr	35.6[a]	31.9[c]	3.7	23.5
LiI	-	44.6[c]	-	24.4
NaF	25.6[a]	21.9[c]	3.7	21.4
NaCl	36.2[a]	32.1[c]	4.1	23.4
NaBr	41.9[a]	40.8[c]	1.1	24.1
NaI	45.6[a]	47.7[c]	-2.1	24.5
KF	33.3[a]	30.4[c]	2.9	23.1
KCl	41.3[a]	38.7[c]	2.6	24.1
KBr	48.2[a]	45.6[c]	2.6	24.4
KI	52.3[a]	51.6[c]	0.7	24.6
RbF	40.2[a]	38.3[c]	1.9	24.2
RbCl	48.1[a]	45.9[c]	2.2	24.4
RbBr	54.1[a]	51.8[c]	2.3	24.6
RbI	59.0[a]	56.7[c]	2.3	24.7
CsF	41.4[a]	-	-	-
CsCl	50.0[a]	47.0[c]	3.0	24.5
CsBr	60.5[a]	51.1[c]	9.4	24.6
CsI	65.0[a]	55.2[c]	9.8	24.7
Rocksalt				
MgO	13.4[b]	9.6[d]	3.8	15.3
FeO	28.8[b]	21.2[d]	7.6	20.8
SrO	27.2[b]	23.8[d]	3.4	21.9
CaO	19.9[b]	15.2[d]	4.7	18.8
CoO	26.5[b]	-	-	-
MnO	29.9[b]	19.2[d]	10.7	20.3
NiO	19.0[b]	25.6[d]	-6.7	21.6

Table 1 – *continued*

Materials and Structures	$S_{experimental}$	S_{Debye}	($S_{experimental}$ - Debye)	$C_{V_{Debye}}$
Wurtzite				
BeO	7.07[b]	5.48[d]	1.59	10.8
ZnO	21.8[b]	23.8[d]	-2.0	21.5
Rutile				
TiO_2	16.8[b]	12.1[d]	4.7	16.8
SnO_2	17.4[b]	17.3[d]	0.1	19.7
GeO_2	-	1.23[d]	-	17.0
SiO_2	9.24[b]	9.16[d]	0.08	14.3
Corundum				
α-Al_2O_3	10.2[b]	7.9[d]	2.3	13.5
α-Cr_2O_3	16.2[b]	12.3[d]	3.9	17.0
α-Fe_2O_3	17.5[b]	16.2[d]	1.3	19.4
Spinel				
Fe_3O_4	20.8[b]	15.9[d]	4.9	19.0
γ-Fe_2SiO_4	18.8[b]	15.8[e]	3.0	18.6
γ-Mg_2SiO_4	-	10.7[e]	-	15.8
$MgAl_2O_4$	11.5[b]	10.5[d]	1.0	15.7
$FeAl_2O_4$	15.2[b]	13.8[d]	1.4	17.7
γ-Ni_2SiO_4	-	13.7[e]	-	17.7
γ-Mg_2GeO_4	-	2.8[e]	-	17.4
γ-Mn_2GeO_4	-	18.4[e]	-	19.9
α-SiO2				
α-SiO_2	13.8[b]	18.5[d]	-4.7	20.5
α-GeO_2	18.5[a]	28.9[e]	-10.4	23.0
Olivine				
α-Mg_2SiO_4	13.6[b]	12.7[e]	0.9	17.3
α-Fe_2SiO_4	21.2[b]	19.7[e]	1.5	20.4
α-Ni_2SiO_4	-	15.9[e]	-	19.0
α-Mg_2GeO_4	-	16.0[e]	-	19.1
α-Mn_2GeO_4	-	21.0[e]	-	21.0
Feldspar				
$NaAlSi_3O_8$	15.9-16.8[b] (low)(high)	19.6[e]	-2.8	20.6
Pyroxene				
$NaAlSi_2O_6$	13.3[b]	13.2[e]	0.1	17.4
$MgSiO_3$	13.5[b]	12.9[e]	0.6	17.5
$FeSiO_3$	18.9[b]	18.3[e]	0.6	20.0
Miscellaneous				
Coesite	13.5[b]	14.9[e]	-1.4	18.5
Calcite	18.5[b]	20.5[c]	-2.0	20.8
Perovskite				
$CaTiO_3$	18.7[b]	12.9[f]	5.8	17.41
$MgSiO_3$	-	8.58[f]	-	14.1

[a] *Landolt-Börnstein Zahlenwerte und Funktionen aus Physik, Chemie, Astronomie, Geophysik, und Technik*, 1961. Sechste Auflage II. Band, Eigenshaften der Materie in ihren Aggregatzuständen, 4. Teil kalorishe zustandsgrössen, Springer-Verlag, Berlin.

[b] Helgeson, H. C., Delaney, J. M., Nesbitt, H. W. & Bird, D. K., 1978. Summary and critique of thermodynamic properties of the rock forming minerals, *Am. J. Sci.*, **278A**, 1–229.

[c] Simmons, G. & Wang, H., 1971. *Single Crystal Elastic Constants and Calculated Aggregate Properties: a Handbook*, MIT Press, Cambridge, Massachusetts.

[d] Chung, D. J., 1974. General relationships among sound speeds: I. New experimental information, *Phys. Earth planet. Int.*, **8**, 113.

[e] Shaw, G. H., 1976. Calculation of entropies of transition and reaction and slopes of transition and reaction lines using Debye theory, *J. geophys. Res.*, **81**, 3031.

[f] Liebermann, R. C., Jones, L. E. A. & Ringwood, A. E., 1977. Elasticity of aluminate, titanate, stannate and germanate compounds with the perovskite structure, *Phys. Earth planet. Int.*, **14**, 165.

whereas the highest optical mode frequencies are on the order of 1100 cm^{-1}. Therefore, near room temperature a Debye model reflects the weak coupling between tetrahedra and predicts saturation of modes at too low a temperature. NaCl, on the other hand, has acoustic and optical mode frequencies that slightly overlap. This might be anticipated since for NaCl acoustic phonon propagation and optical modes are sensitive to the same nearest neighbour interaction. The net effect is that calculated and measured entropies are in better agreement for NaCl than for α-SiO_2. It is plausible to expect that thermodynamical properties of closely packed polyatomic crystals are more likely to be reasonably represented by a Debye model than are properties of more open structures that can contain more internal vibrational modes. The values of $S_{exp}-S_{Debye}$ in Table 1 and discussed below further illustrate this point; they decrease in magnitude in the sequence α-quartz, coesite, and stishovite.

Equation (1) has been used to calculate entropies of a number of materials at room temperature and pressure, and these results and experimental values are tabulated in Table 1. Measured and theoretical entropies are plotted in Fig. 1. Note that values are normalized to entropy per gram atom to facilitate comparison between different crystals (Brady & Stout 1978, 1980). A line with a slope of unity and an offset of 1.7 J/K gm atom may be fitted to these points. When some anomalous solids discussed below are excepted, the specific equation is $S_{Debye} = 0.99\,S_{exp} - 1.67$ with a standard deviation 2.0 J/K gm atom and correlation coefficient $r = 0.9$. These calculations were also carried out using a standard one-frequency Debye model. Although a similar trend emerged, the theoretical values had nearly twice the scatter with respect to measured values. Neither model has adjustable parameters; the better fit of the two-frequency model presumably results from a slightly more realistic description of vibrational structure.

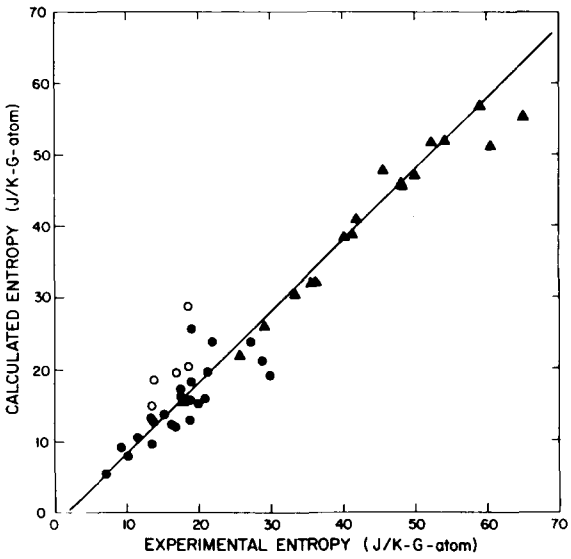

Figure 1. Measured entropies per gram atom compared to those calculated from a Debye model using two cut-off frequencies. Open circles: framework and open-structure silicates; solid triangles: alkali halides; solid circles: others.

In general, measured entropies are larger than Debye entropies. This is to be expected since other contributions to crystalline disorder in addition to very low frequency vibrational terms (Kieffer 1979a, b, 1980) have been omitted. The offset implies an average 'structural' entropy term of the order 1.7 J/K gm atom. Since the offset is independent of characteristic temperatures (as shown by the range of heat capacities in Table 1) it is likely that entropies calculated for mantle materials at high temperature and pressure will be equally well described.

Exceptions to the average behaviour in Table 1 provide further clues to the validity of the Debye model; these exceptions are omitted from the straight-line fit. First, low coordination (open structure) solids tend to have acoustic entropies in excess of thermodynamic measurements. Examples include framework silicates (quartz and albite), coesite, GeO_2 in α-quartz structure, calcite, and ZnO. The acoustic model suggests that all modes are nearer to saturation than is the case since the highest frequency optical modes are not activated at room temperature. Kieffer (1979a) discussed and illustrated the use of the Debye model in greater detail and concluded that complex crystals containing a variety of atomic interactions are not well described by the Debye model.

The transition metal monoxides also exhibit anomalous behaviour. Magnetic disordering is an explanation for the additional entropy of FeO, MnO, and CoO since the Neel temperature for these antiferromagnetic solids lies below room temperature. The excess entropy for a totally disordered magnetic system is $S = kN \ln 2 = 5.78$ J/K mole. While this contribution is important in understanding calculations of Table 1, magnetic order–disorder is not likely to affect entropy calculations for the Earth's mantle because petrological models do not require much iron (or other transition metals) relative to non-magnetic magnesium and silicon.

Nickel oxide is magnetically ordered at room temperature and has a much lower measured entropy than the other disordered, transition metal oxide; also its Debye entropy is much larger than the measured value because low elastic-wave velocities resulting from domain wall movement produce higher Debye entropy (Huntington 1958). Data of Notis, Spriggs & Hahn (1971) suggest that velocities increase above the Neel temperature. To be consistent with Debye calculations, velocities appropriate for equation (1) should be those related to interatomic forces rather than those modified by macroscopic effects (domain wall-stress wave interactions, porosity, etc.).

Adiabatic temperature profiles

Adiabatic temperature profiles for the Earth's interior provide an idealization of a complex situation. However, a nearly adiabatic profile is likely in a convective system (Tozer 1972; O'Connell 1976; Davies 1977; Elsasser, Olsen & Marsh 1979). Further, a first-order model of an adiabatic profile allows calculations of second-order corrections.

A temperature profile that produces constant S_{Debye} can be calculated. As is true for most other thermal models for the Earth, this method ignores defect terms, entropy of mixing and explicit anharmonicity. Input parameters consist of the following: (1) earth model data–density and elastic properties in the calculations are from the Parametric Earth Model, PEM (Dziewonski, Hales & Lapwood 1975). The 'smoothness' of PEM results in less-noisy thermodynamic properties. On the other hand, since PEM lacks a transition layer, D'', at the base of the mantle, it is not possible to calculate temperatures across a suspected boundary layer (e.g. Doornbos & Mondt 1979; Karato 1980). (2) Assumed mean atomic weights – we use values of $\bar{m} = 21.1$ and 49.3 g, for the mantle and core, respectively (Watt, Shankland & Mao 1975). The value for the core is that for dominantly iron composition alloyed with sulphur or oxygen. Results are insensitive to reasonable variations of this parameter; at a maximum it would be 55.9 g for pure iron. (3) A thermal boundary condition is also

necessary and we examine reference temperatures of 1400, 1600, 1800 and 2000°C at 670 km in the expectation that this point will become tied to laboratory observations of mineral phase changes. Our preferred curve is that for $T(670\,\text{km}) = 1600°\text{C}$; this is close to an observed transition in material of olivine composition (Akaogi & Akimoto 1979) at a pressure near 200 kb.

In the calculation a temperature is assigned at a given depth, and entropy is calculated from the Debye model in equation (1) using velocities and densities from PEM. At another (deeper) depth a new temperature is found that produces the same S_{Debye}. Discontinuities are treated by letting the temperature be constant across the boundary and finding a new entropy for the lower layer. We did not attempt a more elaborate, but model-dependent approach to discontinuities. As mentioned, the choice of a smooth seismic model together

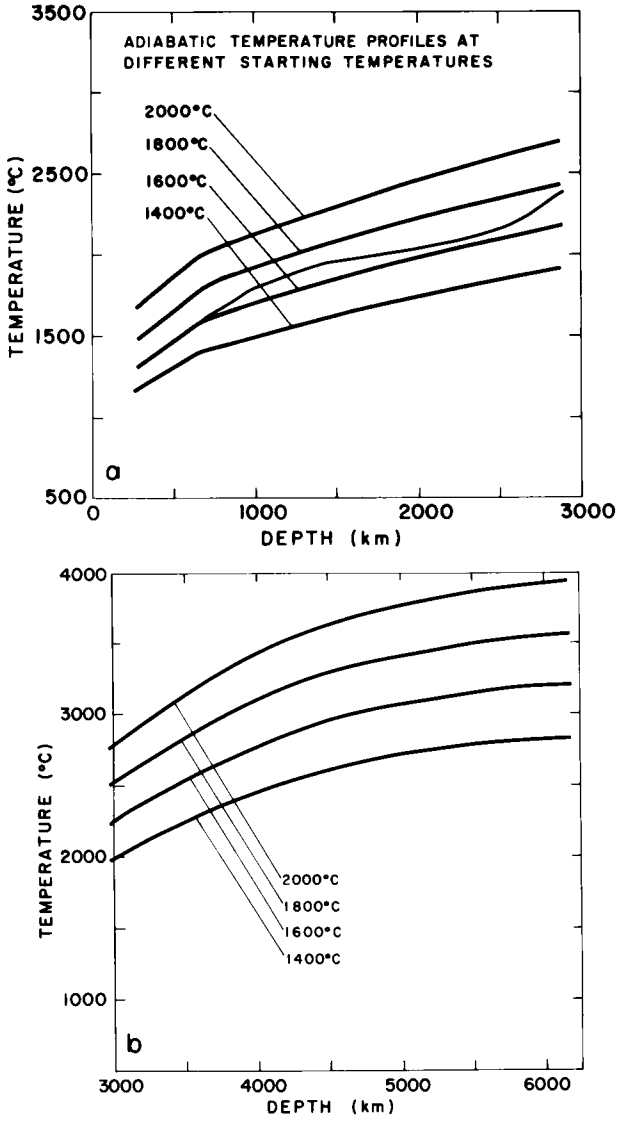

Figure 2. Adiabatic temperature profiles (a) in the mantle and (b) in the core. The curves have been constructed for the four different indicated temperatures at 670 km depth. The second curve beginning at 1600°C and 670 km includes the calculated superadiabatic contribution.

with the treatment of discontinuites makes higher-order effects such as a thermal boundary layer difficult to perceive.

In the outer core all vibrational degrees of freedom are treated as longitudinal. However, calculated thermal properties of the 'liquid' outer core on the assumption of a single Einstein frequency related to the bulk modulus produce the same thermodynamic parameters and temperature profile. There is of course little reason to expect the inner core to have an adiabatic temperature profile, but we have treated it as if it has since, as is shown later, PEM

Table 2. (a) Thermodynamic parameters in the mantle. (b) Thermodynamic parameters in the core.

2a. Depth (km)	Temp. (K)	Thermal Expansion (K^{-1})	Entropy (J/K-gm-atom)	Specific Heat (J/K-gm-atom)	γ_{sa}	γ_a
270	1588	6.83E-05	51.68	24.60	2.09	2.19
320	1626	6.70E-05	51.68	24.60	2.13	2.22
370	1664	6.65E-05	51.68	24.60	2.18	2.26
420	1702	6.61E-05	51.68	24.60	2.24	2.32
470	1736	5.68E-05	49.78	24.54	2.31	2.02
520	1770	5.56E-05	49.78	24.54	2.29	2.01
570	1804	5.43E-05	49.78	24.54	2.27	2.00
620	1839	5.36E-05	49.78	24.55	2.26	1.99
670	1873	5.30E-05	49.78	24.55	2.26	1.99
771	1908	2.19E-05	46.69	24.44	1.29	1.31
871	1941	2.09E-05	46.69	24.44	1.27	1.29
971	1973	1.98E-05	46.69	24.44	1.25	1.27
1071	2004	1.91E-05	46.69	24.44	1.24	1.25
1171	2034	1.83E-05	46.69	24.44	1.23	1.24
1271	2064	1.74E-05	46.69	24.44	1.20	1.21
1371	2092	1.67E-05	46.69	24.44	1.19	1.20
1471	2120	1.60E-05	46.69	24.44	1.17	1.18
1571	2147	1.55E-05	46.69	24.44	1.17	1.16
1671	2174	1.47E-05	46.69	24.44	1.14	1.14
1771	2199	1.43E-05	46.69	24.43	1.13	1.13
1871	2225	1.35E-05	46.69	24.43	1.10	1.10
1971	2249	1.31E-05	46.69	24.43	1.09	1.09
2071	2273	1.25E-05	46.69	24.43	1.06	1.07
2171	2296	1.21E-05	46.69	24.43	1.06	1.06
2271	2319	1.17E-05	46.69	24.43	1.04	1.05
2371	2341	1.12E-05	46.69	24.43	1.02	1.02
2471	2363	1.08E-05	46.69	24.43	1.00	1.01
2571	2384	1.04E-05	46.69	24.43	.99	.99
2671	2405	1.00E-05	46.69	24.43	.97	.98
2771	2426	9.59E-06	46.69	24.43	.94	.96
2871	2446	9.24E-06	46.69	24.43	.93	.95
2885	2449	9.52E-06	46.69	24.43	.95	.96

2b. Depth (km)	Temp. (K)	Thermal Expansion (K^{-1})	Entropy (J/K-gm-atom)	Specific Heat (J/K-gm-atom)	γ_{sa}	γ_a
2971	2505	1.32E-05	51.64	24.66	1.66	1.68
3071	2570	1.28E-05	51.64	24.66	1.68	1.69
3171	2631	1.23E-05	51.64	24.66	1.67	1.69
3271	2691	1.18E-05	51.64	24.66	1.67	1.69
3371	2748	1.14E-05	51.64	24.66	1.67	1.69
3471	2803	1.10E-05	51.64	24.66	1.66	1.68
3571	2856	1.06E-05	51.64	24.66	1.65	1.66
3671	2906	1.02E-05	51.64	24.66	1.64	1.65
3771	2953	9.81E-06	51.64	24.66	1.62	1.63
3871	2998	9.51E-06	51.64	24.66	1.61	1.62
3971	3041	9.13E-06	51.64	24.66	1.58	1.60
4071	3082	8.86E-06	51.64	24.66	1.57	1.58
4171	3119	8.41E-06	51.64	24.66	1.52	1.53
4271	3155	8.12E-06	51.64	24.66	1.50	1.51
4371	3187	7.77E-06	51.64	24.66	1.46	1.47
4471	3218	7.48E-06	51.64	24.66	1.43	1.44
4571	3246	7.02E-06	51.64	24.66	1.36	1.37
4671	3271	6.68E-06	51.64	24.66	1.32	1.33
4771	3294	6.29E-06	51.64	24.66	1.26	1.26
4871	3315	5.94E-06	51.64	24.66	1.20	1.21
4971	3333	5.38E-06	51.64	24.66	1.10	1.10
5071	3348	4.94E-06	51.64	24.66	1.02	1.02
5154	3359	4.55E-06	51.64	24.66	.94	.94
5171	3362	6.60E-06	68.72	24.81	1.37	1.40
5271	3382	7.33E-06	68.71	24.81	1.51	1.52
5371	3399	6.97E-06	68.71	24.81	1.45	1.45
5471	3416	7.43E-06	68.71	24.81	1.54	1.54
5571	3430	6.92E-06	68.72	24.81	1.44	1.46
5671	3442	7.15E-06	68.72	24.81	1.49	1.50
5771	3453	7.09E-06	68.72	24.81	1.48	1.49
5871	3463	6.84E-06	68.72	24.81	1.43	1.44
5971	3470	7.23E-06	68.72	24.81	1.51	1.52
6071	3476	6.95E-06	68.72	24.81	1.46	1.48
6171	3480	6.77E-06	68.72	24.81	1.42	1.42
6271	3483	7.87E-06	68.72	24.81	1.64	1.66
6371	3484	7.64E-06	68.72	24.81	1.59	1.62

presents no seismic evidence for significant departure from adiabatic, homogeneous self-compression.

The resulting temperature profile and thermodynamic properties so determined are labeled with subscript 'sa'; this refers to the adiabatic acoustic model used. Temperatures for several adiabats using different reference temperatures at 670 km are shown in Fig. 2; thermodynamic properties are given in Table 2, both for illustration and to provide a complete tabulation in one place.

It is characteristic of Debye functions such as (1) or (2) that they depend only on ratios θ_p/T and θ_s/T. When a single Debye temperature given by $\theta_D^{-3}=(\theta_p^{-3}+2\theta_s^{-3})/3$ is used, then the simplest model for isentropes is one for which θ_D/T is constant. Our iterative calculation using (1) and (2) gives a temperature increase across the lower mantle that is approximately 10 per cent greater than that from the simpler single temperature model because the compressional modes are relatively unsaturated; T/θ_p is only 1.1 whereas T/θ_D is about 1.9. However, a consequence of the approximation $\theta/T=$ constant is the ready appreciation that any adiabatic temperature profile depends to first order on velocity structure and only weakly on density.

Grüneisen's parameter in the Earth

Although the Debye model is a harmonic model, the Grüneisen parameter, which is an anharmonic property, can be determined through the volume dependence of harmonic modes. This is the quasi-harmonic approximation (Liebfried & Ludwig 1961) and is the usual approach to anharmonicity in solids. This is the only anharmonicity considered in the following calculations.

It is possible to use an adiabatic temperature profile to calculate the thermodynamic Grüneisen's parameter in the Earth. The thermodynamic Grüneisen parameter is given by

$$\gamma_{th} \equiv \frac{\alpha K_s}{\rho c_p} \tag{3}$$

where α is the volume coefficient of thermal expansion, K_s the adiabatic incompressibility, ρ the density, and c_p the heat capacity per unit mass.

Manipulation of these quantities provides the alternative formulation

$$\gamma_{th} = \left(\frac{\partial \ln T}{\partial \ln \rho}\right)_s. \tag{4}$$

For an adiabatic temperature profile $T_s(z)$ we have the result

$$\gamma_{th} = \left(\frac{\partial \ln T_s}{\partial \ln \rho}\right)_s = K_s \frac{d \ln T_s}{dP}. \tag{5}$$

This approach through an adiabatic temperature profile is analogous to current laboratory methods of determining γ from adiabatic decompression using (4) (Ramakrishnan *et al.* 1978; Boehler *et al.* 1979).

As an approximation for the true adiabatic profile we use the adiabatic acoustic profile $T_{sa}(z)$ previously calculated to define a Grüneisen's parameter

$$\gamma_{th} \equiv \left(\frac{\partial \ln T_{sa}}{\partial \ln \rho}\right)_s = K_s \frac{d \ln T_{sa}}{dP}. \tag{6}$$

The adiabatic acoustic Grüneisen's parameter γ_{sa} is plotted in Fig. 3. As is internally consisent with the model, γ_{sa} is temperature-independent; the same curve for γ_{sa} is obtained for all the T_{sa} curves of Fig. 2.

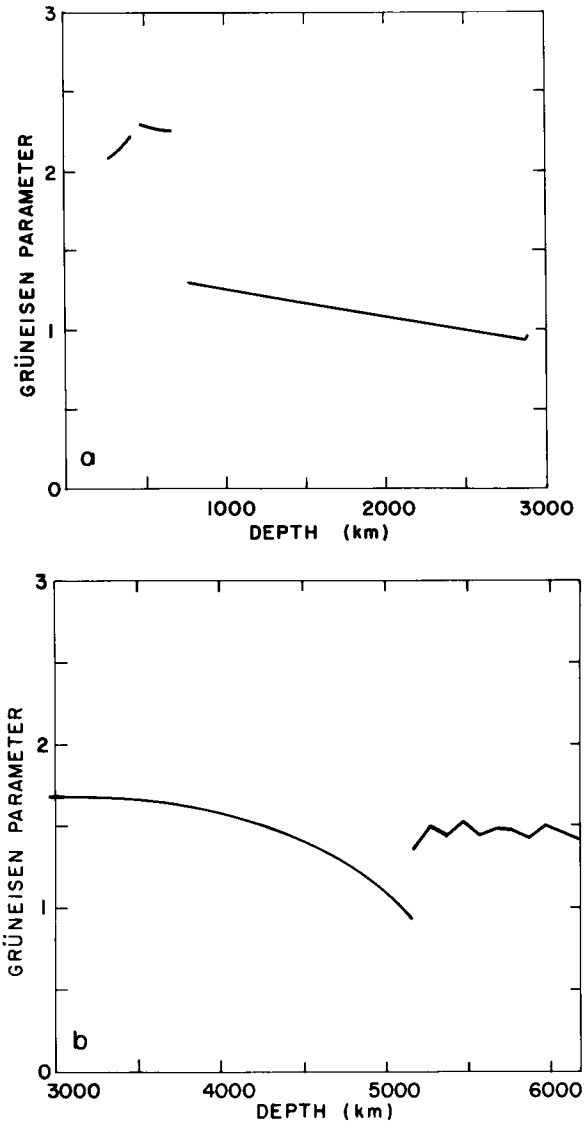

Figure 3. Thermal Grüneisen paramater γ_{sa} calculated (a) for the mantle below 270 km depth and (b) for the core. Variations such as that at the base of the mantle and in the inner core arise from small variations in differentiation of the earth model.

As a calculation of γ_{th} the parameter γ_{sa} contains the uncertainty of any calculation that relies solely on acoustic modes to obtain thermodynamic quantities (Kieffer 1979a). However, this is the only information available for the Earth, and it is not the purpose of this paper to relate γ_{sa} to other definitions of γ because such calculations involve either a detailed description of normal modes (e.g. Striefler & Barsch 1976) or of the details of interatomic potentials (e.g. Irvine & Stacy 1975; Mulargia 1978) in the several kinds of crystals of a composite medium.

It is appropriate to use an adiabatic profile in equations (5) or (6) regardless of the true profile because this choice is consistent with the definition (equation 4) of γ_{th}. Any

additional non-adiabatic gradient dT_{ns}/dz that might otherwise appear in equations (5) or (6) would contribute to the calculated γ but be inconsistent with this definition.

If we assume that $\gamma_{th} = \gamma_{sa}$ then the thermal expansion within the Earth can be calculated from equation (3) in the form

$$\alpha = \frac{\gamma_{sa} \rho \, c_V/(\bar{m} K_s)}{1 - \gamma_{sa}^2 \rho \, T \, c_V/(\bar{m} K_s)} . \tag{7}$$

Here c_V is the specific heat per gram atom and $\bar{m}$ is the mean atomic weight $\simeq$ 21.1 g/gm atom for the mantle (Watt *et al.* 1975) and 49.3 for the core. Even with uncertainties in the approximation for γ_{sa} and in inferences about composition, it is probable that α as plotted in Fig. 4 is correct to 20–30 per cent for the lower mantle. In the upper mantle we might expect α to be greater than that of minerals under room conditions because of the large temperature effect on thermal expansion (e.g. Hazen 1976). However, it is more likely that both γ_{sa} and α are too large in this region owing to effects of inhomogeneity discussed later.

In the previous discussion no explicit anharmonic contributions were included. At sufficiently high temperatures ($T > \theta$) phonon amplitudes are large and the assumption of independent harmonic oscillators becomes less justifiable. The thermodynamics of materials described by (1) and (2) must be altered to include explicit anharmonic contributions. Wallace (1972) showed that up to nearly $3/2\theta_D$, corrections to the harmonic entropy and heat capacity are linear in temperature, on the order of 1 per cent, and can be either positive or negative. Temperatures in the lower mantle are approximately $2\theta_D$ (Anderson *et al.* 1980) Thus, with a modest extrapolation beyond $3/2\theta_D$, we feel that results of Table 2(a) are unlikely to be in error by more than several per cent owing to neglect of explicit anharmonic contributions.

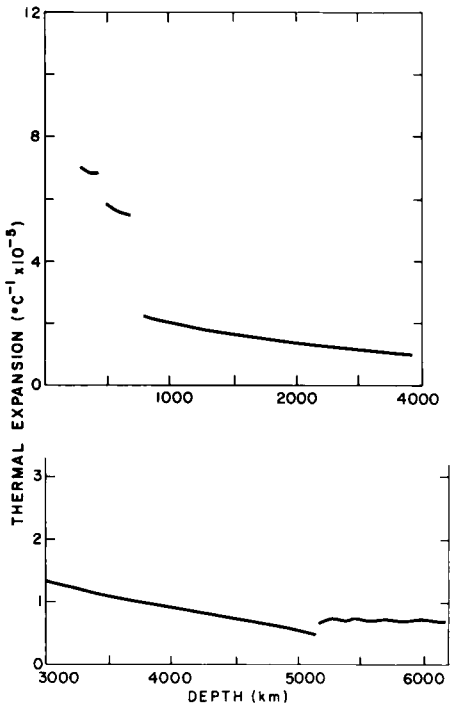

Figure 4. Calculated thermal expansion coefficient in the mantle (above) and in the core.

In the core where $T \gg \theta$ less negligible changes are expected. Stevenson (1980) noted that lattice heat capacities for liquid metals can be less than the classical value by 15 per cent or more. On the other hand, electronic contributions can increase heat capacity (Jamieson, Demarest & Schiferl 1979) so that the net correction to an isentropic calculation such as this one is uncertain. While these effects oppose each other, the calculated temperature difference across the outer core of order 1000 K must be regarded as uncertain to a few hundred degrees.

Effects of inhomogeneity

For the adiabatic density differential in equation (6) we use

$$d \ln \rho|_s = d\rho/\rho|_s = dP/K_s. \tag{8}$$

rather than the measured density differential $d\rho/\rho|_e$ for the Earth obtained from seismic density profiles; K_s is calculated at each depth from seismic velocities and density at that depth. Density profiles in the real Earth can arise from non-adiabatic gradients, changes of phase or composition, and uncertainties in the density profiles themselves, whereas (5) or (6) requires only the adiabatic term.

The difference $d\rho/\rho|_e - dP/K_s$ is a measure of departure from the Adams-Williamson requirement for a homogeneous earth. The true compression $d\rho/\rho|_e$ over a depth interval can depart considerably from that expected on the basis of adiabatic self-compression as seen in Fig. 5; in this circumstance, using $d\rho/\rho|_e$ to calculate γ introduces considerable error. In Fig. 5 the dimensionless parameter

$$\Delta \equiv \left(\frac{\Delta\rho}{\rho} - \frac{\Delta P}{K_s}\right) \Big/ \frac{\Delta P}{K_s} = \frac{\Delta\rho}{\Delta P}\frac{K_s}{\rho} - 1 \tag{9}$$

has been plotted for the Earth for PEM (Dziewonski *et al.* 1975). The quantity Δ is the inhomogeneity parameter $\eta - 1$ defined by Bullen (1975, chapter 11). If an effective incompressibility $K_e \equiv \rho(\Delta P/\Delta\rho)$ is defined for the Earth, we see that $\Delta = (K_s/K_e - 1)$. The physical meaning of Δ is more obvious than that of $\eta = -(V_p^2 - 4/3V_s^2)\rho g\, d\rho/dr$; here g = acceleration of gravity and r = radius. When Δ differs from zero, it is an indication of strong variations from the adiabatic condition so that T_{sa} probably departs strongly from the true profile. As seen in Fig. 5 this condition prevails in the upper mantle above 670 km. The large Δ for the 420–670 km region indicates a greater-than-adiabatic compression suggestive of phase changes, and γ_{sa} is subject to greater uncertainty. Above 420 km Δ is large and negative as would be consistent with the presence of conductive heat losses leading to a superadiabatic geotherm. The smoothing effect of PEM is most pronounced in the inner core. Masters (1979) showed that in this region Δ (or the parameter η) increases substantially for Models 1066A and 1066B (Gilbert & Dziewonski 1975), which may indicate compositional change. However, it should be borne in mind that present seismic data weakly constrain Δ in the lower mantle (to ± 0.05 according to Masters 1979) and almost not at all in the inner core and upper mantle (Masters 1979, private communication).

We have found no inconsistencies using the real Earth densities to calculate an adiabatic temperature profile. Equation (4) may be rewritten as

$$\left.\frac{dT}{T}\right|_s = \gamma \left.\frac{d\rho}{\rho}\right|_s. \tag{10}$$

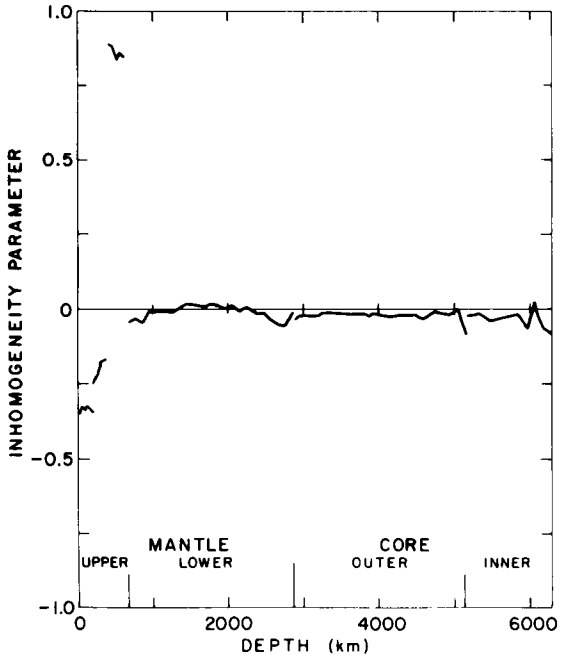

Figure 5. Deviations from adiabatic self-compression in the Earth as expressed by the parameter $\Delta = (K_s/K_e - 1)$. Values greater than zero indicate compression more rapid than that in a homogeneous adiabatic material, e.g. as a region of phase changes; negative values indicate a rate of compression less than adiabatic as should be caused by thermal expansion from a conductive, superadiabatic contribution to the thermal gradient.

For small values of Δ an error term in the adiabatic temperature gradient may be expressed using (9) as

$$\delta\left(\frac{dT}{T}\right)_s = -\gamma\frac{dP}{K_s}\Delta. \tag{11}$$

Since $(dP/K_s)\Delta \ll \Delta\rho/\rho$ and $\gamma \sim 1$ the error term is small. An equivalent correction was made, and the calculated temperatures and thermodynamic properties were little changed; entropy values change by 10^{-2} J/K gm atom, and temperatures differ by tenths of degrees.

As previously observed (Davies & Dziewonski 1975; Butler & Anderson 1978) the Earth below 670 km closely fits the Adams-Williamson requirement. An overall, slightly negative Δ would suggest a superadiabatic gradient needed to maintain convective motion. While Masters' (1979) calculations of $\eta = 1 + \Delta$ indicate that Δ cannot be significantly constrained to this precision, this Δ may be qualitatively correct; it is worthwhile to pursue the implications of its use, if only as indication of what can be gained from more refined seismic data at a later time. Thus, a maximum, spherically symmetrical superadiabatic temperature ΔT_{na} can be calculated by equating the difference $\Delta\rho/\rho|_e - \Delta P/K_s$ to the volume thermal expansion $-\alpha\Delta T_{na}$, where thermal expansivity α was calculated from equation (7). The integrated ΔT_{na} for the lower mantle is 203°C compared to a ΔT_{sa} of 575°C, for $T(670\,\text{km}) =$ 1600°C, while that for the outer core is 404°C compared to a ΔT_{sa} of 985°C. Again, note that because of smoothing, this model can only poorly include any thermal boundary layers apart from the non-adiabatic gradient itself.

If adiabatic and non-adiabatic contributions over the lower mantle–outer core are added, the total temperature difference is about 2200°C. This amount added to a presumed 1600°C

at 670 km yields a temperature at the inner–outer core boundary of 3800°C, in reasonable agreement with Stacey's (1977) estimate of 4000°C. This temperature is still indeterminate in this model because conductive losses in the metallic outer core would tend to decrease the gradient and a thermal boundary layer at the core–mantle interface would raise it (Jeanloz & Richter 1979).

We have added the non-adiabatic gradient ΔT_{na} to the 1600°C isentrope in Fig. 2. It is interesting that ΔT_{na} has the S-like shape expected for a laterally averaged temperature profile in a convecting mantle; Jeanloz & Richter (1979) summarized the evidence for this shape. While the result may disappear with better seismic profiles, it does suggest the temperatures – with smoothed features – to be expected in a lower mantle that convects independently of the upper mantle and with little flow across the 670 km discontinuity (Jeanloz & Richter 1979). Note that since ΔT_{na} results from integration of Δ, it is not so susceptible to error as Δ itself.

Table 2 compares γ_{sa} with the acoustic Grüneisen parameter in the Earth. The acoustic parameters are defined as

$$\gamma_{ai} \equiv \left(\frac{\partial \ln V_i}{\partial \ln \rho}\right)_T + 1/3. \tag{12}$$

At high temperatures

$$\gamma_a = (\gamma_p + 2\gamma_s)/3 \tag{13}$$

where $i = p, s$ for compressional and shear velocities (Anderson *et al.* 1968). However, since the adiabatic and isothermal elastic constants are equal to within a few per cent we have used

$$\gamma_i = \left(\frac{\partial \ln V_i}{\partial \ln \rho}\right)_s + 1/3 = K_s \frac{d \ln V_i}{dP} + 1/3. \tag{14}$$

This definition should still be better than that which is frequently used for the Earth, $\gamma_i = (\partial \ln V_i)/(\partial \ln \rho)_e + 1/3$, in regions where Δ is large.

The agreement between γ_{sa} and γ_a (Table 2) is to be expected. However, while γ_{sa} is not restricted to high temperatures, equation (13) is valid only for $T > \theta$. In the lower mantle $T \simeq \theta$ so that gram atomic heat capacity values in Table 2 are percentibly less than the classical value of 24.94 J/K gm atom. The deviation is due to the relatively lower occupation of compressional modes.

In regions where Δ is appreciable, the γ_a used here is lower than the γ_a derived when $\Delta\rho/\rho|_e$ used instead of dP/K_s, e.g. about 2.7 above 420 km instead of 2.2. However, this difference is purely due to the definition of differential density; γ_{sa} and γ_a agree when the same differential density is used for their calculation. In 'homogeneous' regions of low Δ all the calculated γ's agree to within a per cent or two although even the volume dependence of γ_a is slightly affected as discussed below.

Volume dependence of Grüneisen's parameter

The volume dependence of Grüneisen's parameter has long been of theoretical interest and of use in reducing data from shock wave compression measurements. Fig. 6 displays this dependence for the mantle and core; atomic volume was calculated using the above assumption that $\bar{m}$ for the mantle and core are 21.1 and 49.3 g/gm atom, respectively. Uncertainties

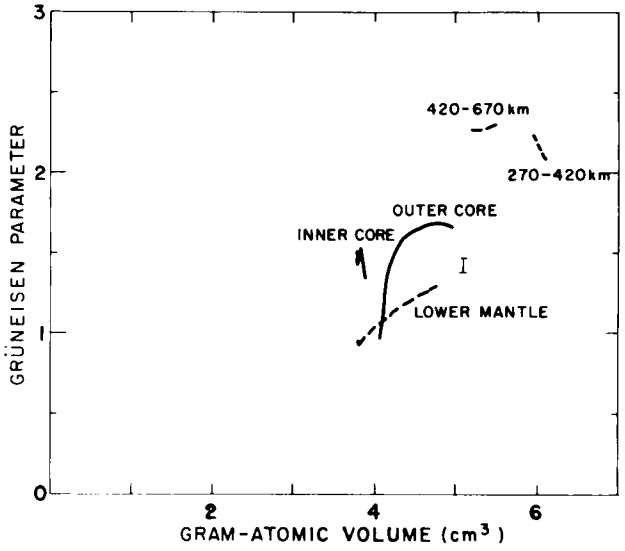

Figure 6. Volume dependence of thermal Grüneisen parameter γ_{sa} for assumed mean atomic weights of 21.1 g for the mantle and 49.3 g for the core. Different mean atomic weights would slightly change the locations of the curves, but not their trends.

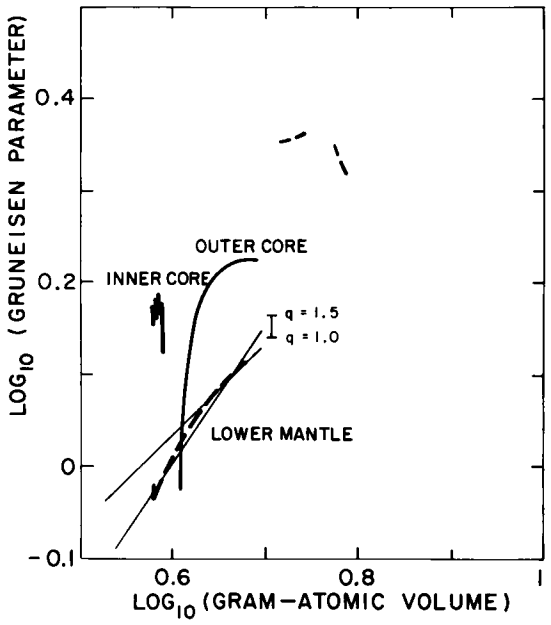

Figure 7. Log–log plot of γ_{sa} versus gram atomic volume to test the power-law relationship. Slopes corresponding to exponents $q = 1$ and 1.5 are shown. The vertical bar indicates the range of Grüneisen parameters extrapolated from the central mantle to a zero-pressure density of 4.15 g cm^{-3} using q in the range 1–1.5.

in $\bar{m}$ are of the order of 5 per cent (Watt *et al.* 1975); relative variations are probably still less and are unlikely to seriously affect the results. The plot includes the origin in order to make it easy to compare these results with predictions of the form

$$\gamma/\gamma_0 = (V/V_0)^q = (\rho_0/\rho)^q. \tag{15}$$

Fig. 7 provides an additional check of this relationship. A first-order conclusion from these figures is that present models of the Earth afford limited hope of confirming simple volume dependences of the form equation (15), even allowing for possible differences between γ_{sa} and other definitions of γ.

Only in the lower mantle do both the quality of seismic velocity and density resolution and the adherence to the Adams-Williamson condition of adiabatic self-compression seem adequate to apply to equation (15). On both figures we have used the density $\rho_0 = 4.15$ Mg m^{-3} that comes from extrapolation to zero pressure using third-order finite strain theory (Davies & Dziewonski 1975) of lower mantle compression curves. Density and γ_{sa} at 1071 km were used to calculate γ_{sa} from equation (13). The concave-downward curve results from using an adiabatic density change (8) rather than the real Earth value (Anderson 1979a). It may preclude an aesthetic fit, but errors associated with using equation (15) may not be too serious in practice (Anderson 1979a; Stacy 1977).

Conclusions

The entropies of simple closely packed solids were shown to match calculated values based on a two-frequency Debye model. The success of this harmonic model lends justification for its use in calculating isentropic temperature profiles in the Earth's interior. This approach through isentropic profiles reverses the more common calculation through equations of state. However, the reverse procedure gives results not unlike those stated by others who use the usual forward approach from equation of state theory. The entropy calculations have some visible omissions: anharmonicity beyond that contained in the quasi-harmonic model, defect contributions and mixing contributions. However, these are ordinarily also omitted in the forward calculations where they are equally significant, but the omissions are not so apparent.

Using calculated isentropies from PEM, we derived the Grüneisen parameter and thermal expansion coefficient. A thermodynamic γ close to the acoustic γ is suggested with γ roughly equal to 1 in the lower mantle and 1.7 in the outer core. The thermal expansion coefficient α is close to 10^{-5} K^{-1} in the lower mantle and core. Small deviations from a truly isentropic density profile are interpreted as resulting from non-adiabatic contributions to the thermal gradient. A temperature of 3800°C at the inner–outer core boundary results from addition of adiabatic and non-adiabatic contributions; because it excludes the effect of boundary layers it is therefore a lower limit.

Acknowledgments

We are grateful to O. L. Anderson, G. Masters, R. Merrill, J. Shaner and a conscientious, ascerbic reviewer for constructive comments. This work was supported by the Division of Basic Energy Sciences in the Department of Energy under contract W-7405-ENG-36.

References

Akaogi, M. & Akimoto, S., 1979. High-pressure equilibria in a garnet lherzolite with special reference to Mg^{2+} – Fe^{2+} partioning among constituent minerals, *Phys. Earth planet. Int.*, **83**, 31–51.

Anderson, O. L., 1979a. The high-temperature acoustic Grüneisen parameter in the Earth's interior, *Phys. Earth planet. Int.*, **18**, 221–231.

Anderson, O. L., 1979b. Evidence supporting the approximation $\gamma\rho$ = const for the Grüneisen parameter of the earth's lower mantle, *J. geophys. Res.*, **84**, 3537–3542.

Anderson, O. L., Schreiber, E., Liebermann, R. & Soga, N., 1968. Some elastic constant data in minerals relevant to geophysics, *Rev. Geophys.*, **6**, 491–524.

Boehler, R., Skoropanev, A., O'Mara, D. & Kennedy, G. C., 1979. Grüneisen parameter of quartz, quartzite and fluorite at high pressures, *J. geophys. Res.*, **84**, 3527–3531.

Brady, J. B. & Stout, J. H., 1978. Gram-atom units for convenience and insight, *EOS, Trans. Am. geophys. Un.*, **59**, 394.

Brady, J. B. & Stout, J. H., 1980. Normalizations of thermodynamic properties and some implications for graphical and analytical problems in petrology, *Am. J. Sci.*, **280**, 173–189.

Brillouin, L., 1953. *Wave Propagation in Periodic Structures*, Dover, New York.

Bullen, K. E., 1975. *The Earth's Density*, Chapman & Hall, London.

Butler, R. & Anderson, D. L., 1978. Equation of state fits to the lower mantle and outer core, *Phys. Earth planet. Int.*, **17**, 147–162.

Davies, G. F., 1977. Whole-mantle convection and plate tectonics, *Geophys. J.*, **49**, 459–486.

Davies, G. F. & Dziewonski, A. M., 1975. Homogeneity and constitution of the Earth's lower mantle and outer core, *Phys. Earth planet. Int.*, **10**, 336–343.

Doornbos, D. J. & Mondt, J. C., 1979. *P* and *S* waves diffracted around the core and the velocity structure at the base of the mantle, *Geophys. J. R. astr. Soc.*, **57**, 381–395.

Dziewonski, A. M., Hales, A. L. & Lapwood, E. R., 1975. Parametrically simple Earth models consistent with geophysical data, *Phys. Earth planet. Int.*, **10**, 12–48.

Elsasser, W. M., Olson, P. & Marsh, B. D., 1979. The depth of mantle convection, *J. geophys. Res.*, **84**, 147–155.

Gilbert, F. & Dziewonski, A., 1975. An application of normal mode theory to the retrieval of structural parameters and source mechanisms from seismic spectra, *Phil. Trans. R. Soc. A*, **278**, 187–269.

Hazen, R. M., 1976. Effects of temperature and pressure on the crystal structure of forsterite, *Am. Mineral.*, **61**, 1280–1293.

Hazen, R. M., 1977. Temperature, pressure, and composition: structurally analogous variables, *Phys. Chem. Miner.*, **1**, 83–94.

Hazen, R. M. & Finger, L. W., 1979. Bulk modulus-volume relationship for cation-anion polyhedra, *J. geophys. Res.*, **84**, 6723–6728.

Huntington, H. B., 1958. *The Elastic Constants of Crystals*, Academic Press, New York.

Irvine, R. D. & Stacey, F. D., 1975. Pressure dependence of the thermal Grüneisen parameter with application to the Earth's lower mantle and outer core, *Phys. Earth planet. Int.*, **11**, 157–165.

Jamieson, J. C., Demarest, H. H. & Schiferl, D., 1978. A reevaluation of the Grüneisen parameter for the Earth's core, *J. geophys. Res.*, **83**, 5929–5935.

Jeanloz, R. & Richter, F. M., 1979. Convection, composition and the thermal state of the lower mantle, *J. geophys. Res.*, **84**, 5497–5504.

Jorgensen, J. D., 1978. Compression mechanisms in α-quartz structures – SiO_2 and GeO_2, *J. appl. Phys.*, **49**, 5473–5478.

Karato, S., 1980. Low Q zone at the base of the mantle: evidence for lower mantle convection, *Phys. Earth planet. Int.*, **22**, 155–161.

Kieffer, S. W., 1979a. Thermodynamics and lattice vibrations of minerals: 1. Mineral heat capacities and their relationships to simple lattice vibrational models, *Rev. Geophys. Space Phys.*, **17**, 1–19.

Kieffer, S. W., 1979b. Thermodynamics and lattice vibrations of minerals: 2. Vibrational characteristics of silicates, *Rev. Geophys. Space Phys.*, **17**, 20–34.

Kieffer, S. W., 1980. Thermodynamics and lattice vibrations of minerals: 4. Application to chain, sheet and orthosilicates, *Rev. Geophys. Space Phys.*, **18**, 862–886.

Liebfried, G. & Ludwig, W., 1961. Theory of anharmonic effects in crystals, in *Solid State Physics*, **12**, 275–444, eds Seitz, F. & Turnbull, D., Academic Press, New York.

Mao, H. K., 1968. The pressure dependence of the lattice parameters and volume of ferromagnesian spinels, and its applications to the Earth's mantle, *PhD dissertation*, University of Rochester, Rochester, New York.

Mao, N. H., 1974. Velocity-density systematics and its implications for the iron content of the mantle, *J. geophys. Res.*, **79**, 5447–5452.

Masters, G., 1979. Observational constraints on the chemical and thermal structure of the Earth's deep interior, *Geophys. J. R. astr. Soc.*, **57**, 507–534.

Mulargia, F., 1978. Is the common definition of the Mie-Grüneisen equation of state inconsistent?, *Geophys. Res. Lett.*, **4**, 590–592.

Notis, M. R., Spriggs, R. M. & Hahn, W. C. Jr, 1971. Elastic moduli of pressure-sintered nickel oxide, *J. geophys. Res.*, **76**, 7052–7061.

O'Connell, R. J., 1975. On the scale of mantle convection, *Tectonophys.*, **38**, 119–136.

Ramakrishnan, J., Boehler, R., Higgins, G. H. & Kennedy, G. C., 1978. Behavior of Grüneisen's parameter of some metals at high pressures, *J. geophys. Res.*, **83**, 3535–3538.

Shankland, T. J., 1972. Velocity-density systematics: derivation from Debye theory and the effect of ionic size, *J. geophys Res.*, 77, 3750–3758.

Shaw, G. H., 1976. Calculation of entropies of transition and reaction and slopes of transition and reaction lines using Debye theory, *J. geophys. Res.*, **81**, 3031–3035.

Smith, R. A. 1969. *Wave Mechanics of Crystalline Solids*, Chapman & Hall, London.

Stacey, F., 1977. A thermal model of the Earth, *Phys. Earth planet. Int.*, **15**, 341–348.

Stevenson, D. J., 1980. Applications of liquid state physics to the earth's core. *Phys. Earth planet. Int.*, **22**, 42–52.

Striefler, M. E. & Barsch, G. R., 1976. Elastic and optical properties of stishovite, *J. geophys. Res.*, **81**, 2453–2466.

Tozer, D. C., 1972. The present thermal state of the terrestrial planets, *Phys. Earth planet. Int.*, **6**, 182–197.

Wallace, D. C., 1972. *Thermodynamics of Crystals*, Wiley, New York.

Watt, J. P., Shankland, T. L. & Mao, N. H., 1975. Uniformity of mantle composition, *Geology*, **3**, 91–94.